ARTICLE

Charge Separation from the Bursting of Bubbles on Water

Indrani Bhattacharyya, Joshua T. Maze, George E. Ewing,* and Martin F. Jarrold*

Chemistry Department, Indiana University, 800 East Kirkwood Avenue, Bloomington, Indiana 47405, United States

ABSTRACT: Film droplets formed from the bursting of 2.4 mm diameter bubbles on the surface of pure water are predominantly negatively charged. The charge generated per bubble varies chaotically; a few bubbles generate more than -3×10^6 elementary charges (e) but the vast majority generate much less. The average is -5×10^4 e/bubble, and it is not significantly affected by bubbling rate or temperature. The charge diminishes with increasing salt concentration and vanishes for concentrations above 10^{-3} M. We propose a mechanism consistent with the observed charge separation. The model relies on the assumption that the surface of pure water has a slight excess of hydroxide ions. The charge separation results when water with entrained counterions (H_3O^+) flows out of the thinning film of the bubble cap, leaving behind the excess OH^- on the surface. Addition of salt reduces the Debye length, and the charge separation mechanism becomes less effective as the Debye length becomes small compared with the film thickness. The excess charge near the surface of pure water is very small, around -4 nC/m^2.
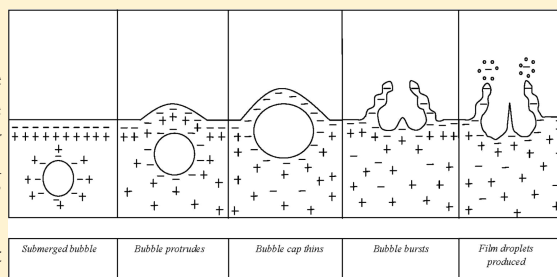
1. INTRODUCTION

Splashing,[1,2] bubbling,[3−10] spraying,[11,12] boiling,[13] freezing,[14−19] and dripping,[20,21] processes that disrupt the surface of water, lead to charge separation and electrification. Water drops formed from breaking of a water surface can be charged either positively or negatively, depending on their size and method of generation.

Electrically charged water drops play a significant role in many natural phenomena. The most obvious example is the lightning associated with thunderstorms, tornadoes, and active volcanoes.[4,15] An exotic case is the perpetual lightning surrounding the mouth of Rio Catatumbo as it spills into Lago de Maracaibo,[22] the largest lake in South America. A more accessible example is waterfall electrification where in certain regions of the Austrian Alps, discharges can be observed.[23] Of more general meteorological significance is wave action over lakes and oceans that produces electrified drops[3−5,8,10] and contributes significantly to the positively charged atmosphere.

The phenomenon of water electrification has drawn to its study Franklin,[24,25] Volta,[4] Faraday,[4] Peltier,[4] Rayleigh,[26] Kelvin[20,21] and a host of other scientists from the 18th, 19th, and 20th centuries, yet many questions remain about the mechanism of charge separation. An early model offered by Lenard[27] to account for the negative mist at the base of waterfalls involved the rupture of the electrical double layer of ions proposed to exist at the water interface.[28] One of the impediments to understanding this general phenomenon is the uncertain nature of the water interface.[29−31] Here, techniques coming to maturity in the 21st century are filling out the picture. In particular, advanced surface-selective nonlinear optical spectroscopies[32−37] and ab initio and classical molecular dynamics (MD) calculations[35,38−44] together, are beginning to yield images of the interface on a molecular scale.

With special attention to the role of the air−water interface, the focus of this paper is the study of charge separation that occurs as bubbles burst at the surface of water.

The hydrodynamic behavior of water, as a bubble bursts, is an elegantly choreographed process well studied by others.[3,4,45−52] In brief, equilibrium between the buoyancy of the bubble and surface tension determines the extent of its protrusion above the water surface and, hence, the area of the exposed bubble cap. The bubble cap (or film), separating the air inside from outside, thins as the water drains down. Finally the cap ruptures, flinging micrometer-sized[4,8] airborne film droplets into a horizontal trajectory above the surface of water. A cavity at the water surface is left after the bubble bursts. Water then rushes into this cavity to fill the void, forming a jet as the mass of water gathers from the sides and pushes upward. This jet then breaks into a series of larger droplets (typically one-tenth of the size of the bubble[4,7,8]) that are ejected vertically, several cm into the air.[8]

Using the Millikan oil drop method, Blanchard measured positive charge on the jet droplets formed on the bursting of air bubbles both in natural and artificial seawater.[5,53] Experiments with distilled water, however, gave erratic results.[5] Iribarne and Mason, who did not distinguish between jet droplets and film droplets, measured negative charges from bubble bursting in pure water and a few salt solutions.[54]

In this paper, we separate the jet droplets from the film droplets to measure the charge on the film droplets exclusively. We choose purified water to start and then apply the method to aqueous salt solutions.

2. EXPERIMENTAL SECTION

The design of our experiment was directed at achieving three goals: to separate film droplets from the jet droplets, to measure
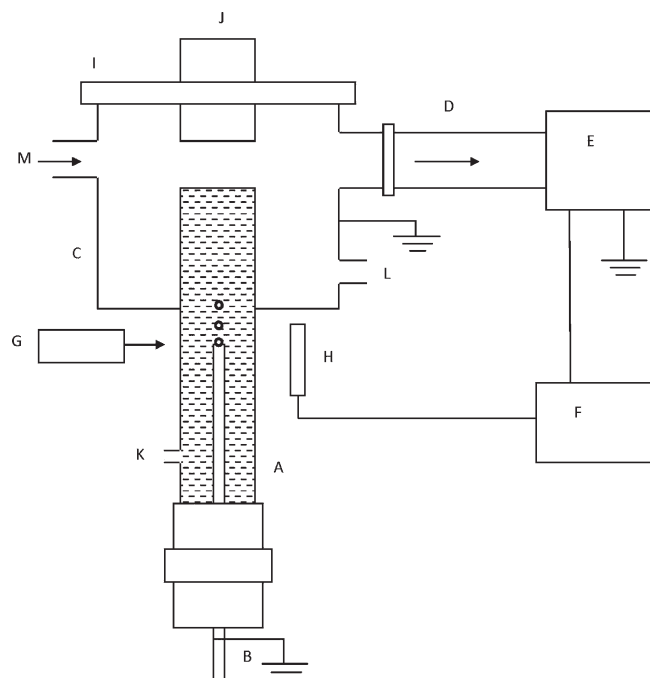
Figure 1. Experimental apparatus for bubble generation and charge detection. Key to labels in the figure: (A) water chamber, (B) capillary, (C) droplet chamber, (D) film droplet transfer tube, (E) charge detector, (F) oscilloscope, (G) laser, (H) photodiode, (I) chamber cover, (J) jet droplet trap, (K) water inlet, (L) water outlet, and (M) nitrogen inlet to droplet chamber.

the charge on the film droplets, and to maintain chemical purity of the water and the bubbling gas.

Our apparatus for generating bubbles and measuring charge is shown in Figure 1. The water is contained in a quartz tube (A) equipped with a stainless steel capillary (1.2 mm i.d.) (B) through which UHP nitrogen (Airgas, Inc.) is flowed to form bubbles. The bubble diameter (which is controlled by the diameter of the capillary[4,8,58]) is around 2.4 mm. The bubbling rate is fixed by controlling the nitrogen flow with a leak valve. The rate of bubble formation is measured by a He−Ne laser (G) and a photodiode (H). The stainless steel droplet chamber (C) is attached to the upper part of the quartz tube. Nitrogen is flowed through this chamber to purge CO_2 from the system. Purified water (resistivity 18.2 MΩ cm) at room temperature ($\sim$20 °C), flowing from a Millipore Academic A10 unit, is then introduced at inlet (K) and leaves at outlet (L). The quartz tube was flushed regularly with water to remove any opportunist impurities.

The droplet chamber (C) is covered by a stainless steel plate (I). The plate is electrically insulated from the chamber by a Teflon O-ring. The center of the plate has a hollow stainless steel cylinder (J) attached that is filled with steel wool to collect the jet droplets. The water generating the film droplets did not make contact with the steel wool. The left port (M) on the droplet chamber is used to introduce nitrogen above the water surface to sweep the film droplets into a stainless steel transfer tube (D). The transfer tube is 50 cm long and 3.8 cm diameter. Film droplets are carried into the transfer tube by a 200 cm^3/s flow of nitrogen gas. The tube is wrapped with electrical tape, and the carrier gas, which enters at $\sim$20 °C, is heated to $\sim$60 °C during transit through the tube. Sufficient time is provided for the film droplets to evaporate to yield small ions before reaching the detector (E). The identity of the ions is unknown, but they are
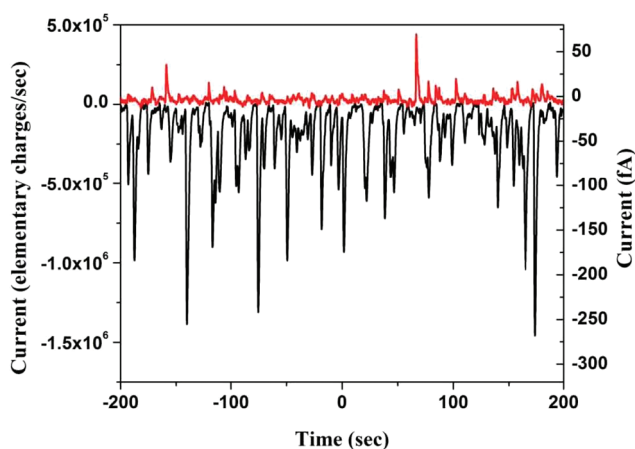
Figure 2. Typical traces for positive (red) and negative (black) currents recorded with a bubbling rate of 1 bubble/s. The traces were recorded using the oscilloscope, and they have been smoothed with a fast Fourier transform to remove the high-frequency components of the electrical noise.

probably $H_3O^+(H_2O)_N$ and $OH^-(H_2O)_N$ with N small or zero. The gas flow, the diameter of the transfer tube, and the density and viscosity of nitrogen at 60 °C correspond to a Reynold's number (Re) of 410. Since Re < 1900, the turbulence is suppressed,[55] and the resulting laminar flow prevents the film droplets from hitting the wall of the transfer tube on the way to the detector. Under these conditions, the average transit time is 2.8 s.

The detector, an air-ion counter (Alphalab, Inc.), is a current measuring device. It operates by sampling the air that flows through the unit. It can measure either positive or negative ions separately through internal collector plates. The unit was calibrated by applying known currents to the detector plate. The output from the air-ion counter was connected to an oscilloscope (Tektronix DPO 3054) (F).

The capillary, the droplet chamber, the chamber cover, and the transfer tube were grounded to eliminate induced currents. The metal parts in the apparatus act as a Faraday cage, reducing interference from external electric fields.

Since the only significant source of charges in pure water is the very low concentration ($\sim$10^{-7} M) of hydroxide and hydronium ions, great care was taken to exclude other ions. CO_2, which acidifies the water and introduces HCO_3^- ions,[54] was eliminated by using UHP nitrogen (Airgas) as the bubbling gas and also by purging the system beforehand with the same nitrogen gas. All the joints were sealed with O-rings to avoid air-borne contamination.

3. RESULTS

Background current measurements (both positive and negative) were taken with the nitrogen flowing above the water surface but in the absence of bubbling. The resulting root-mean-square noise, 4 fA, corresponds to a detection limit of 125 ions/cc·s.

Typical traces expressed both as numbers of elementary charges/s and currents (fA) for both negative and positive measurements at 1 bubble/s are shown in Figure 2. The negative and positive charge measurements were taken during different bubbling sequences, since our detector can only measure one polarity at a time. The traces were recorded with the oscilloscope and smoothed by a fast Fourier transform (FFT) to remove high-frequency electrical noise. We used a cutoff frequency of 2.5 Hz, which is small
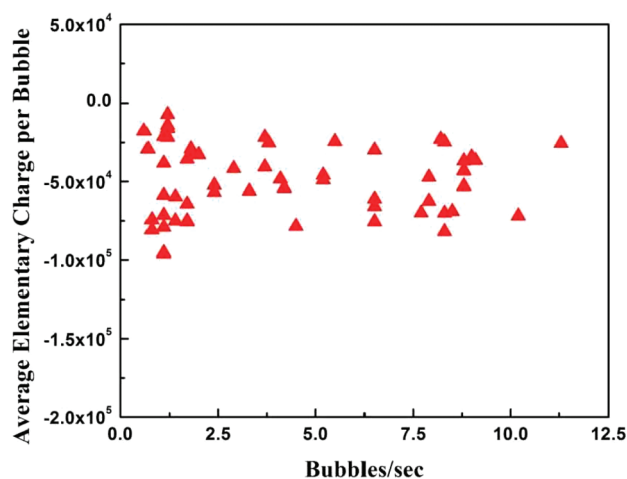
Figure 3. The average number of negative elementary charges per bubble obtained in a 400 s run plotted against the bubbling rate.

Figure 4. The average negative charge per bubble plotted against the LiI concentration. The scale at the top of the plot shows the Debye length.

enough that the FFT does not significantly perturb the amplitudes or profiles of the main features in the trace.

We identify two key features of these measurements. First, the current is produced in a chaotic pattern. A fraction of negative current appears as surges manifested within 20 or so randomly spaced, well-resolved, sharp features, all with uniform full width of 2 s at half-maximum. Other current surges are expressed in 50 or so overlapping features. There are also 5 or so positive current surges which are significant. It is clear that the majority of the 400 bubble burst events do not give rise to well-defined surges of current. Second, the total negative current far exceeds the positive current. Integration of the negative current trace over 400 s yields -7.3×10^7 elementary charges (e) whereas the positive trace integrates to $+1.2 \times 10^7$ e, or only 16% of the total negative charge.

Other measurements at a rate of 1 bubble/s gave traces similar to those in Figure 2, but the charge measurements fluctuate widely. We explored this for a range of bubbling rates up to 11/s. The average negative charge per bubble vs bubbling rate is plotted in Figure 3. We find fluctuations in charge up to a factor of 5 for each bubbling rate. Such large fluctuations are consistent with a previous study.[54] The spread in the charge per bubble seems to be higher in cases of lower bubbling rates than for higher bubbling rates. However, the average for each bubbling rate is independent of the bubbling rate. The overall average negative charge, obtained by averaging over all the measurements, is -5×10^4 e/bubble. The positive charge shows similar fluctuations, although the positive charge is always less than the negative. The average positive charge was found to be $+8 \times 10^3$ e/bubble.

To investigate whether the charge separation in bubble bursting can be influenced by an electric field at the surface of water, ±30 V was applied to the chamber cover (I) (Figure 1). No significant effect was observed on either the positive or negative charge per bubble. A voltage applied to the water through the capillary did not affect the charge separation significantly, either.

Charge separation, typically measured at 20 °C, was not affected by variations in temperature from 18 to 25 °C. The accuracy in temperature measurement was ±0.5 °C.

Charge separation from bubbling in lithium iodide (LiI) solutions was studied for concentrations from 10^{-7} to 0.5 M. As in the case of pure water, several-fold variations in charge were observed from run to run. The results shown in Figure 4 are
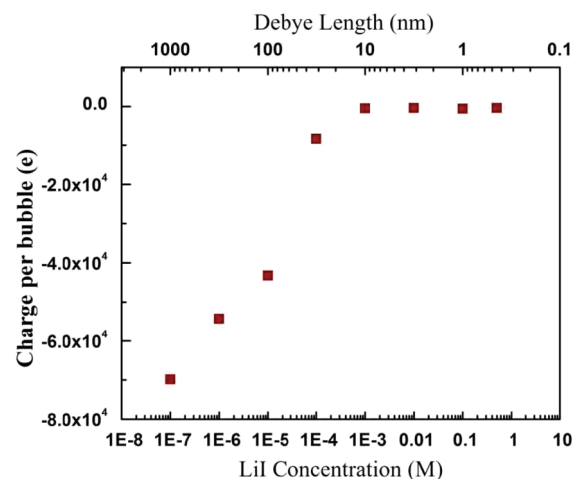
averages. For 10^{-3} M and above, no charge separation was observed. A significant amount of negative charge started appearing at 10^{-4} M and became more negative toward 10^{-7} M. The average measurement per bubble at 10^{-7} M LiI of -7×10^4 e is within the range expected for pure water. The magnitude of the positive charge was substantially less (<15%) than the magnitude of the negative charge observed for each individual run, as for the case of pure water.

4. DISCUSSION

4.1. Generation of Bubbles and Film Droplets. The method for producing bubbles of a specific size by the use of carefully prepared fine glass capillary tips was first described by Blanchard.[4,7,56] In accordance with his observation, our capillary with an i.d. of 1.2 mm produces bubbles with a diameter around 2.4 mm. Upon rupture, the cap of a bubble with this diameter is expected to yield an average of around 6 film droplets with an average diameter of 25 μm.[57]

The number of film droplets generated per bubble burst is known to vary widely.[51,57] It is reasonable to expect that there is a correlation between the number of film droplets generated and the amount of charge separation, and so the wide variation in number of film droplets could be responsible for the chaotic charging behavior reported here. The peaks in the current traces (see Figure 2) would then result from bubble bursting events that yield large numbers of film droplets.

4.2. Charge Separation in Neat Water. The 20 or so well-resolved negative current surges in Figure 2 reveal a full-width of 2 s at half-maximum, consistent with the transit time of the film droplets to the detector. We now assume each of these surges arise from a single bubble burst. We integrate the largest of these negative surges to obtain $q = -3 \times 10^6$ e. Analysis of the maximum positive surge yields $q = +8 \times 10^5$ e. There may be other bubble bursting events that lead to a larger charge separation. However, we take these values for the analysis to follow.

The only charges available in pure (pH 7) water are OH^- and H_3O^+ ions, both at concentrations of 6×10^{19} m^{-3}. The bubble cap thickness just before rupture has been estimated to be around 350 nm for a 2.4 mm diameter bubble,[51] so if there were no adjustment of the OH^- and H_3O^+ concentrations on the formation of the bubble cap, it would contain, on average, around 1.8×10^8 OH^- ions and an equal number of H_3O^+ ions. The negative

| Submerged bubble | Bubble protrudes | Bubble cap thins | Bubble bursts | Film droplets produced |
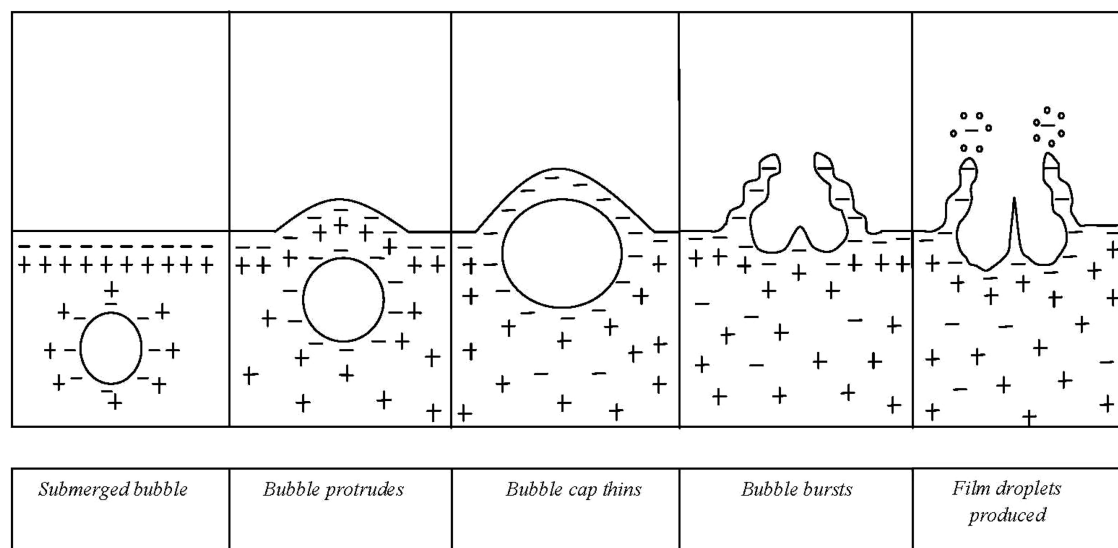
Figure 5. Schematic diagram showing the charge separation model discussed in the text.

charge we have measured cannot be the result of a random fluctuation in the number of these ions, as a statistical analysis shows. If a droplet contains n charges and the probability that each charge is $+$ or $-$ is 0.5, then the standard deviation (σ) for the excess charge is $(n/4)^{1/2}$. With 1.8×10^8 anions and the same number of cations, $\sigma = 9.5 \times 10^3$. This value is much too small to account for either the negative ($-3 \times 10^6\,e$) or positive ($8 \times 10^5\,e$) extremum observed. The expected average deviation from the mean[12] is $(n/2\pi)^{1/2}$, which is $\pm 7.6 \times 10^3\,e$ for the pure water bubble cap considered here. This value is substantially smaller than the average negative charge per bubble ($-5 \times 10^4\,e$) but comparable to the average positive charge per bubble ($8 \times 10^3\,e$).

An alternative explanation posits, for the large negative charge we observe, either an enhancement of OH^- ions or a depletion of H_3O^+ ions within the bubble cap before it bursts, producing film droplets. We have developed a model to account for this charge separation.

4.3. The Model. A five-step process to describe our model is laid out in Figure 5.

1. Submerged bubble. Two nitrogen−water interfaces are presented. One belongs to the submerged bubble, and the other to the bulk water. We assume each surface has a slight excess of hydroxide ions, consistent with several experiments on the surface charge of water[58−61] (although at variance with other experiments[32,62] and some calculations[62]). A neighboring interior region of hydronium ions assumes the neutrality of the water. In our figure, the ions are represented by − and + signs.

2. Bubble protrudes. The bubble is buoyed to the water surface. As it moves upward, water in the boundary layer is squeezed out, carrying with it the interior hydronium ions.

3. Bubble cap thins. The bubble cap thins, leaving the two interfaces enriched in hydroxide ions. Eventually, the bubble cap is pierced. The cap is ∼350 nm thick at this point, according to recent estimates.[51]

4. Bubble bursts. The opening enlarges and gathers the film's mass into a toroidal ring, which starts to break up into beads[51] as it collapses toward the water surface.

5. Film droplets produced. The beads on the toroidal ring continue to grow, and eventually, the beads convert into film droplets by a filament breaking mechanism. On average, around 6 film droplets[57] are formed with average diameters around 25 μm.

Although the negative charge on the film droplets can be explained by the proposed model, the process responsible for the small positive charge is not clear. As we have already shown, it cannot be the result of random fluctuations. We propose another explanation here. The positive film droplets may be charged by induction during their production by the filament breaking mechanism. In this explanation, a primary, negatively charged film droplet breaks off together with a smaller secondary film droplet that is positively charged through induction.[63]

While an excess of negative charge is being carried away from the bulk water in the form of film droplets, the bulk water must be left with an excess of positive charge. These excess positive charges in water have to be neutralized by accepting electrons from the metal capillary by the following reaction:[64] $2H_3O^+ + 2e^- \rightarrow 2H_2O + H_2$. Thus, a potential is generated in the water that would lead to an electric field gradient at the interface of the water. Blanchard has reported that an electric field applied over the surface of salt water influences the charge on the jet droplets.[53] In our experiment, however, an applied voltage did not have a significant effect on the charge generated, possibly because the bias applied was insufficient to affect the exceedingly small excess negative charge at the interface. To confirm this, we estimated the excess negative charge at the surface of water.

Previous studies indicate that around 6 film droplets with an average radius of 25 μm are produced from a 2.4 mm diameter bubble burst.[57] Using this information and the volume of the bubble cap, we find that around 12% of the bubble cap is transferred to the film droplets. If we assume that the observed average charge, $-5 \times 10^4\,e$, results from 12% of the bubble-film, we conclude that the excess charge on the surface of the bubble is around -4 nC/m² (1 excess charge per 43 μm²). This is much lower than the excess charge obtained for an oil−water interface from mobility measuments.[65]

4.4. Charge Distribution Measurements in Aqueous Salt Solutions. It has been established by both theoretical studies (MD and MC simulations)[38−40,44] and surface-selective spectroscopic studies (vibrational sum-frequency spectroscopy and second harmonic generation)[32−34,36,37,66−69] that large polarizable ions (such as iodide or bromide) have a surface propensity. For a LiI solution, it is expected that I^- will have a surface propensity and,

5726

dx.doi.org/10.1021/jp102719s |*J. Phys. Chem. A* 2011, 115, 5723–5728

hence, the film droplets might be expected to carry some negative charge. In contrast, our observation (see Figure 4) shows that they are uncharged. The answer to this paradox is revealed by considering the distribution of charges in the water interfacial region.

We imagine excess negative charges (OH^- or I^-) at the water surface. Following the discussion by Israelachvili,[70] the negative surface is compensated by a region of mobile positive ions whose charge density falls off at an electrolyte concentration-dependent decay called the Debye length. For pure water at pH 7 with 10^{-7} M of hydronium and hydroxide ions, the Debye length is 1 μm.[70] A 0.1 M aqueous solution of a 1:1 electrolyte contains 0.1 M of both positive and negative ions and a Debye length of 1 nm. If the Debye length is much less than the film thickness, when the bubble cap thins and liquid flows out, it carries away less positive charge, and thus, when the film bursts, most of the droplets formed will not carry a charge. According to the results shown in Figure 4, charge separation starts to become significant when the Debye distance approaches $10-20$ nm and then increases quickly as the Debye distance increases to become comparable to the value for pure water for a 10^{-7} M salt solution. In the mechanism for charge separation proposed above, charge separation should start to become less effective when the Debye length becomes less than half the terminal film thickness (i.e., at around 200 nm). Thus, the salt dependence of the charge separation displayed in Figure 4 is entirely consistent with the mechanism proposed to account for the charge separation.

The expected random charge fluctuation in the bubble film for an aqueous salt solution is estimated to be $\sim \pm 8 \times 10^5$ for a 10^{-3} M solution, rising to $\pm 8 \times 10^6$ for a 0.1 M solution. Hence, the charge separation found in individual bubble bursting events here (see Figure 4) is much less than the calculated random charge fluctuation, in contrast to pure water.

Although we do not see a charge on film droplets for 0.1 M salt solution, Blanchard observed positive charge on jet droplets from seawater (0.5 M). A different charge separation mechanism must account for the positive charge on the jet droplets from seawater. Further models should include consideration of ion mobilities[71,72] and the possibility of different surface behavior in response to these ions.

5. CONCLUSIONS

In summary, we have measured the charge on the film droplets generated during the bursting of a nitrogen bubble on the surface of pure water and on aqueous salt solutions. The charge is predominantly negative for pure water and for dilute salt solutions, but vanishes for concentrated salt solutions ($>10^{-3}$ M). A mechanism is proposed to account for the charge separation. The formation of a negatively charged film droplet is attributed to a slight enhancement of the OH^- at the surface of pure water. When water flows out of the thinning bubble cap, it carries away the H_3O^+ counterions, leaving the cap with a slight negative charge, and some of this excess charge ends up on the film droplets when the bubble bursts.

The lack of charge on film droplets from concentrated salt solutions is explained by the fact that the Debye length is much smaller than the film thickness, and hence, the charge separation mechanism that occurs with pure water is no longer effective. As the salt concentration decreases, the Debye length increases, and the charge separation process starts to occur. Because the bubble-bursting mechanism involves the breaking of air–water interface, we realize that these findings may provide some insight about the

charge at the air–water interface that has recently become controversial.[29−31,62]

■ AUTHOR INFORMATION

Corresponding Author
*E-mails: (G.E.E.) ewingg@indiana.edu and (M.F.J.) mfj@indiana.edu.

■ REFERENCES

(1) Shewchuk, S. R.; Iribarne, J. V. *Q. J. R. Meteorol. Soc.* **1971**, *97*, 272–282.
(2) Levin, Z.; Hobbs, P. V. *Philos. Trans. R. Soc., A* **1971**, *269*, 555–585.
(3) Blanchard, D. C. *Prog. Oceanogr.* **1963**, *1*, 171–202.
(4) Blanchard, D. C. From Raindrops to Volcanoes. *Adventures with Sea Surface Meteorology*; Dover: Mineola, NY, 2004.
(5) Blanchard, D. C. *J. Atmos. Sci.* **1958**, *15*, 383–396.
(6) Blanchard, D. C. *J. Atmos. Sci.* **1966**, *23*, 449–451.
(7) Blanchard, D. C.; Syzdek, L. D. *Limnol. Oceanogr.* **1978**, *23*, 389–400.
(8) Blanchard, D. C. W., A. H. *Ann. N.Y. Acad. Sci.* **1980**, *338*, 330–347.
(9) Kientzler, C. F.; Arons, A. B.; Blanchard, D. C.; Woodcock, A. H. *Tellus* **1954**, *6*, 1–7.
(10) Cipriano, R. J.; Blanchard, D. C.; Hogan, A. W.; Lala, G. G. *J. Atmos. Sci.* **1983**, *40*, 469–479.
(11) Maze, J. T.; Jones, T. C.; Jarrold, M. F. *J. Phys. Chem. A* **2006**, *110*, 12607–12612.
(12) Zilch, L. W.; Maze, J. T.; Smith, J. W.; Ewing, G. E.; Jarrold, M. F. *J. Phys. Chem. A* **2008**, *112*, 13352–13363.
(13) Armstrong, W. G. Letters to M. Faraday. *Philos. Mag.* **1840**, *XVII*, 370–374.
(14) Mason, B. J.; Maybank, J. *Q. J. R. Meteorol. Soc.* **1960**, *86*, 176–185.
(15) Evans, D. G.; Hutchinson, W. C. A. *Q. J. R. Meteorol. Soc.* **1963**, *89*, 370–375.
(16) Latham, J. *Q. J. R. Meteorol. Soc.* **1964**, *90*, 209–211.
(17) Gill, E. W. B. *Br. J. Appl. Phys.* **1953**, *4*, S16–S19.
(18) Latham, J.; Mason, B. J. *Proc. R. Soc. London, Ser. A* **1961**, *260*, 537–549.
(19) Saunders, C. P. R. *J. Geophys. Res.* **1994**, *99*, 10,773–10,779.
(20) Kelvin, L.; Maclean, M. *Proc. R. Soc. London* **1894**, *56*, 84–94.
(21) Kelvin, L.; Maclean, M.; Galt, A. *Proc. R. Soc. London* **1894**, *57*, 335–346.
(22) Hanbury-Tracy, J. *Geograph. J.* **1944**, *104*, 145–165.
(23) Edward Law, S. *J. Electrost.* **2001**, *51−52*, 25–42.
(24) *Autobiographical Writings*; Franklin, B., Ed.; The Viking Press: New York, 1952.
(25) Franklin, B. *Experiments and Observations on Electricity, made at Philadelphia in America by Benjamin Franklin, L.L.D., and F.R.S.*; Harvard University Press: Cambridge, 1941.
(26) Rayleigh, L. *Proc. R. Soc. London* **1878**, *28*, 405–409.
(27) Lenard, P. *Ann. Phys. (Paris, Fr.)* **1892**, *46*, 584.
(28) Debye P. W.; Huckel, E. *Phys. Z.* **1923**, *24*.
(29) Beattie, J. K. *Phys. Chem. Chem. Phys.* **2008**, *10*, 330–331.
(30) Vacha, R.; Buch, V.; Milet, A.; Devlin, J. P.; Jungwirth, P. *Phys. Chem. Chem. Phys.* **2008**, *10*, 332–333.
(31) Vacha, R.; Buch, V.; Milet, A.; Devlin, P.; Jungwirth, P. *Phys. Chem. Chem. Phys.* **2007**, *9*, 4736–4747.
(32) Petersen, P. B.; Saykally, R. J. *J. Phys. Chem. B* **2005**, *109*, 7976–7980.
(33) Petersen, P. B.; Saykally, R. J. *Annu. Rev. Phys. Chem.* **2006**, *57*, 333–364.
(34) Petersen, P. B.; Saykally, R. J. *J. Phys. Chem. B* **2006**, *110*, 14060–14073.

5727

dx.doi.org/10.1021/jp102719s |*J. Phys. Chem. A* 2011, 115, 5723–5728

(35) Petersen, P. B.; Saykally, R. J.; Mucha, M.; Jungwirth, P. *J. Phys. Chem. B* **2005**, *109*, 10915–10921.

(36) Tarbuck, T. L.; Ota, S. T.; Richmond, G. L. *J. Am. Chem. Soc.* **2006**, *128*, 14519–14527.

(37) Tian, C.; Ji, N.; Waychunas, G. A.; Shen, Y. R. *J. Am. Chem. Soc.* **2008**, *130*, 13033–13039.

(38) Jungwirth, P.; Tobias, D. J. *J. Phys. Chem. B* **2002**, *106*, 6361–6373.

(39) Jungwirth, P.; Tobias, D. J. *J. Phys. Chem. B* **2000**, *104*, 7702–7706.

(40) Jungwirth, P.; Tobias, D. J. *J. Phys. Chem. B* **2001**, *105*, 10468–10472.

(41) Iyengar, S. S.; Day, T. J. F.; Voth, G. A. *Int. J. Mass Spectrom.* **2005**, *241*, 197–204.

(42) Iyengar, S. S.; Petersen, M. K.; Day, T. J. F.; Burnham, C. J.; Teige, V. E.; Voth, G. A. *J. Chem. Phys.* **2005**, *123*, No. 084309-9.

(43) Petersen, M. K.; Iyengar, S. S.; Day, T. J. F.; Voth, G. A. *J. Phys. Chem. B* **2004**, *108*, 14804–14806.

(44) Jungwirth, P.; Tobias, D. J. *Chem. Rev.* **2005**, *106*, 1259–1281.

(45) Boulton-Stone, J. M.; Blake, J. R. *J. Fluid Mech.* **1993**, *254*, 437–466.

(46) Leifer, I.; de Leeuw, G.; Cohen, L. H. *Geophys. Res. Lett.*, *27*.

(47) Iacono, M. J.; Blanchard, D. C. *Atmos. Res.* **1987**, *21*, 139–149.

(48) Spiel, D. E. *J. Geophys. Res.* **1992**, *97*, 11,443–11,452.

(49) Francesca Lugil, F. Z. *Phys. Chem. Chem. Phys.* **2007**, *9*, 2447–2456.

(50) Liebman, I.; Corry, J.; Perlee, H. E. *Science* **1968**, *161*, 373–375.

(51) Spiel, D. E. *J. Geophys. Res. (Oceans)* **1998**, *103*, 24907–24918.

(52) Knelman, F. N. D.; Newitt, D. M. *Nature* **1954**, *173*, 261.

(53) Blanchard, D. C.; Syzdek, L. D. *Limnol. Oceanogr.* **1975**, *20*, 762–774.

(54) Iribarne, J. V.; Mason, B. J. *Trans. Faraday Soc.* **1967**, *63*, 2234–&.

(55) Reynolds, O. *Philos. Trans. R. Soc. London. A* **1895**, *186*, 123–164.

(56) Blanchard, D. C.; Syzdek, L. D. *Chem. Eng. Sci.* **1977**, *32*, 1109–1112.

(57) Wu, J. *J. Phys. Oceanogr.* **2001**, *31*, 3249–3257.

(58) Takahashi, M. *J. Phys. Chem. B* **2005**, *109*, 21858–21864.

(59) Beattie, J. K.; Djerdjev, A. M. *Angew. Chem., Int. Ed.* **2004**, *43*, 3568–3571.

(60) Beattie, J. K.; Djerdjev, A. N.; Warr, G. G. *Faraday Discuss.* **2009**, *141*, 31–39.

(61) Creux, P.; Lachaise, J.; Graciaa, A.; Beattie, J. K. *J. Phys. Chem. C* **2007**, *111*, 3753–3755.

(62) Buch, V.; Milet, A.; Vacha, R.; Jungwirth, P.; Devlin, J. P. *Proc. Natl. Acad. Sci. U S.A.* **2007**, *104*, 7342–7347.

(63) Sanford, F. *Phys. Rev.* **1918**, *11*, 445.

(64) Duffin, A. M.; Saykally, R. J. *J. Phys. Chem. C* **2007**, *111*, 12031–12037.

(65) Beattie, J. K. *Lab Chip* **2006**, *6*, 1409–1411.

(66) Baldelli, S.; Schnitzer, C.; Simonelli, D. *J. Phys. Chem. B* **2002**, *106*, 5313–5324.

(67) Goh, M. C.; Hicks, J. M.; Kemnitz, K.; Pinto, G. R.; Heinz, T. F.; Eisenthal, K. B.; Bhattacharyya, K. *J. Phys. Chem.* **1988**, *92*, 5074–5075.

(68) Gragson, D. E.; McCarty, B. M.; Richmond, G. L. *J. Am. Chem. Soc.* **1997**, *119*, 6144–6152.

(69) Rao, Y.; Comstock, M.; Eisenthal, K. B. *J. Phys. Chem. B* **2006**, *110*, 1727–1732.

(70) Tadmor, R.; Hernandez-Zapata, E.; Chen, N.; Pincus, P.; Israelachvili, J. N. *Macromolecules* **2002**, *35*, 2380–2388.

(71) Chen, H.; Voth, G. A.; Agmon, N. *J. Phys. Chem. B* **2010**, *114*, 333–339.

(72) Knecht, V.; Levine, Z. A.; Vernier, P. T. *J. Colloid Interface Sci.* **2010**, *352*, 223–231.